The Nitrogen Principal Field Gradient Tensor, Bonding, and Barrier to Proton Tunneling in Ethylenimine

M. K. Kemp[1a] and W. H. Flygare[1b]

Contribution from the Noyes Chemical Laboratory, University of Illinois, Urbana, Illinois. *Received May 23, 1968*

Abstract: The high-resolution microwave spectra of ethylenimine and ethylenimine-d_1 have been recorded to obtain the diagonal elements of the ^{14}N nuclear quadrupole coupling constant tensor in both principal inertial axis systems. This information yields the principal field gradient axis system coupling constants of $\chi_{\alpha\alpha} = 0.685 \pm 0.005$ MHz, $\chi_{\beta\beta} = 3.004 \pm 0.09$ MHz, and $\chi_{\gamma\gamma} = -3.689 \pm 0.09$ MHz. The γ axis approximates the C_3 axis of NH_3 and the α axis is in the CNC plane. The principal field gradient axis values are rotated into the CNC molecular plane giving $\chi_{xx} = 0.685 \pm 0.005$ MHz, $\chi_{yy} = 1.77 \pm 0.16$ MHz, $\chi_{zz} = -2.46 \pm 0.16$ MHz, and $\chi_{yz} = 2.59 \pm 0.13$ MHz. The z axis is perpendicular to the ring and the y axis bisects the CNC angle. The planar axis field gradients are used to interpret the local ^{14}N atomic hybrid orbitals. The Walsh model of bonding appears to be the most appropriate description of the electron distribution with an sp^2 system perpendicular to the CNC plane. One sp^2 orbital participates in the NH bond, one orbital contains a lone pair, and the third sp^2 orbital is directed into the ring. A fourth orbital is a pure p function also in the plane of the ring and perpendicular to the sp^2 system. Other hybrid orbitals are examined including an sp^5 in-ring bent bond picture. The N inversion frequency is less than 15 kHz on the basis of a line-width study. A simple barrier model is presented and a convenient formula is given relating the barrier height to the inversion frequency and vibrational energy spacing. The lower limit for the barrier height is consistent with barriers obtained from rate studies in magnetic resonance.

In the previous paper[2a] on the ^{33}S nuclear quadrupole coupling in ethylene sulfide, it was concluded that the Walsh[2b] bonding scheme was more appropriate in describing the local ^{33}S field gradients than the corresponding Coulson–Moffitt[3] scheme. Ethylenimine provides another convenient small ring compound in which the electron distribution at the nitrogen nucleus can be probed by a study of the ^{14}N nuclear quadrupole interaction. Tolles and Gwinn[4] have measured the diagonal elements in the ^{14}N nuclear quadrupole coupling constant tensor in the principal inertial axis system of ethylenimine.

We have reopened the study of ethylenimine in order to measure the principal ^{14}N quadrupole coupling constant tensor elements and determine the orientation of the field gradient tensor relative to the molecular bond axes. The principal or complete field gradient tensor can then be rotated into the bond axis system or into the molecular plane. The field gradients in the molecular plane axis system can be used to interpret the bonding in ethylenimine.

The method used to obtain the principal field gradient axis system and the corresponding tensor elements is to measure the diagonal elements of the field gradient tensor in both ethylenimine and ethylenimine-d_1. The known angle between the two principal inertial axis systems is then used to obtain the off-diagonal element. The complete field gradient tensor in either inertial axis system can be diagonalized to give the principal values and the orientation of the tensor. This analysis also yields some information on the deuterium quadrupole coupling constants. The nitrogen field gradients are used to interpret the bonding in ethylenimine.

In addition, we have also attempted to measure the nitrogen inversion tunneling frequency. A discussion is given relating to the inversion barrier in ethylenimine and a simple formula is derived relating the barrier height to the vibrational energy spacing and tunneling frequency. Lower limits are given for the barrier height in ethylenimine.

Experimental Section

The ethylenimine used in this work was obtained from Matheson Coleman and Bell and was used without further purification. Deuterated ethylenimine was obtained by mixing equal quantities of D_2O and ethylenimine in the liquid phase. All spectra were taken on a 5-kHz Stark modulated spectrograph using phase stabilization of the signal source. The spectrograph and the L-band absorption cell used in this work have been described elsewhere.[5] Three Q-branch transitions were observed in ethylenimine under high resolution. The hyperfine structure was completely resolved. The coupling scheme for a single quadrupolar nucleus with angular momentum, I, coupling with the rotational angular momentum, J, is well known.

$$\mathbf{I} + \mathbf{J} = \mathbf{F}$$

The transitions between the J and F states are shown in Table I. We have fit the two independent ^{14}N coupling constants to the data in Table I by using an available computer program.[6] Our results are $\chi_{aa} = 0.685 \pm 0.005$ MHz, $\chi_{bb} = 2.170 \pm 0.005$ MHz, and $\chi_{cc} = -2.855 \pm 0.005$ MHz. These values compared well with $\chi_{aa} = 0.69 \pm 0.01$ and $\chi_{bb} = 2.170 \pm 0.01$ MHz given by Tolles and Gwinn.[4] The calculated difference frequencies are also listed in Table I.

Four Q-branch transitions were studied in the deuterated species.[7] The analysis of the data was similar to the work in ethylenimine. However, in ethylenimine-d_1 there are two quadrupolar nuclei to consider. Since the ^{14}N nucleus couples more strongly to the rotational angular momentum than the deuteron, the appropriate coupling scheme is

$$\mathbf{I}_N + \mathbf{J} = \mathbf{F}_1$$

$$\mathbf{I}_D + \mathbf{F}_1 = \mathbf{F}$$

(1) (a) University of Illinois Graduate Fellow; (b) Alfred P. Sloan Fellow.

(2) (a) R. L. Shoemaker and W. H. Flygare, *J. Am. Chem. Soc.*, 90, 6263 (1968); (b) A. D. Walsh, *Trans. Faraday Soc.*, 45, 179 (1949).

(3) C. A. Coulson and W. E. Moffitt, *J. Chem. Phys.*, 15, 151 (1947); *Phil. Mag.*, 40, 1 (1949).

(4) W. M. Tolles and W. D. Gwinn, *J. Chem. Phys.*, 42, 2253 (1965).

(5) W. H. Flygare and V. W. Weiss, *ibid.*, 45, 2785 (1966).

(6) P. J. Krusic, Quantum Chemistry Program Exchange, Indiana University, Bloomington, Ind.

(7) T. E. Turner, V. C. Fiora, and W. M. Kendrick, *J. Chem. Phys.*, 23, 1966 (1955).

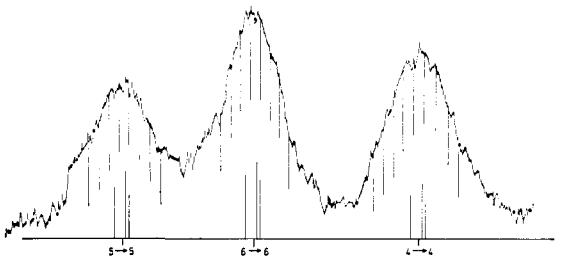

Figure 1. The 5(3,2)→5(5,1) transition in ethylenimine-d_1.

Krusic's program[6] was again used to calculate the frequencies of rotational transitions for the ($I_N JF_1$, $F_1 I_D F$) system. A plotting routine, written for an IBM 7094 computer by J. M. Pochan, was used to display the transition profiles for comparison with experiment. The constants for the ^{14}N nucleus were varied until the splittings, as measured from the computer plots, matched those obtained from experimental spectra. Then the quadrupole coupling constants of the deuterium nucleus were varied in an attempt to match experimental line shapes. The splittings for the five Q-branch transitions observed here are listed in Table II. Only the $F_1 \rightarrow F_1'$ quantum numbers are listed since each $F_1 \rightarrow F_1'$ transition contains the major deuterium hyperfine splittings. This can be seen in Figure 1 where the experimental trace of the 5(3,2)→5(5,1) transition is shown. The stick spectrum given under the spectrum shows the D hyperfine structure in addition to the larger splittings given by ^{14}N. There are a large number of possible transitions which have smaller intensities, but these are not included since they have no detectable effect on the line shape. Each transition in Figure 1 is labeled by the quantum numbers $F_1 \rightarrow F_1'$ according to the coupling scheme given earlier. This analysis leads to the following values: $\chi_{aa}^N = 2.450 \pm 0.005$ MHz, $\chi_{bb}^N = 0.685 \pm 0.005$ MHz, $\chi_{cc}^N = -3.135 \pm 0.005$ MHz, $\chi_{aa}^D < |0.150|$ MHz, $\chi_{bb}^D < |0.150|$ MHz, and $\chi_{cc}^D < |0.300|$ MHz.

Since no splitting due to deuterium nuclear quadrupole coupling was observed in any of the transitions, it is not possible to determine the coupling constants for deuterium exactly. The limits set are consistent with the deuterium coupling constants found in formaldehyde-d_2.[8] The values for formaldehyde are $\chi_{aa}^D = -0.013$, $\chi_{bb}^D = 0.098$, and $\chi_{cc}^D = -0.085$ MHz which approximately corresponds to χ_{aa}^D, χ_{cc}^D, and χ_{bb}^D, respectively, in ethylenimine-d_1 due to similar principal inertial axis systems.

The values used for the stick spectrum in Figure 1 were chosen to illustrate the effect of the deuterium nucleus and should not be taken as exact values.

A *c*-dipole transition, 3(2,1)→3(3,1), in ethylenimine was observed under very high resolution in an attempt to observe the doublet caused by proton tunneling. The transition was seen as a single Lorentzian line shape with minimum half-width at half-height of 12 kHz. This leads us to conclude that the splitting between the lowest two inversion levels is less than 15 kHz since *c*-type transitions should be split by twice the inversion frequency.[9]

Table I. The Calculated and Observed Splittings between $F \rightarrow F'$ Transitions in Ethylenimine

$J \rightarrow J'$	$(F \rightarrow F')_2$–$(F \rightarrow F')_1$	$\nu_2 - \nu_1$, MHz Obsd	Calcd[a]
1(0,1)→1(1,0)	(2→1)–(1→1)	0.207	0.205
	(0→1)–(2→1)	0.310	0.309
	(1→2)–(0→1)	0.343	0.342
	(2→2)–(1→2)	0.208	0.206
	(1→0)–(2→2)	1.089	1.079
2(0,2)→2(1,1)	(3→3)–(2→2)	1.559	1.562
	(1→1)–(3→3)	0.865	0.868
3(2,1)→3(3,1)	(4→4)–(2→2)	0.170	0.172
	(3→3)–(4→4)	0.502	0.491

[a] $\chi_{aa} = 0.685$ MHz, $\chi_{bb} = 2.170$ MHz.

Table II. The Calculated and Observed Splittings between $F \rightarrow F'$ Transitions in Ethylenimine-d_1

$J \rightarrow J'$	$(F_1 \rightarrow F_1')_2$–$(F_1 \rightarrow F_1')_1$	$\nu_2 - \nu_1$, MHz Obsd	Calcd[a]
2(1,2)→2(1,1)	(3→3)–(2→2)	1.233	1.228
	(1→1)–(3→3)	0.692	0.682
3(1,2)→3(3,1)	(4→4)–(3→3)	1.091	1.089
	(2→2)–(4→4)	0.374	0.380
3(2,2)→3(2,1)	(4→4)–(3→3)	0.483	0.489
	(2→2)–(4→4)	0.173	0.175
5(3,2)→5(5,1)	(6→6)–(5→5)	0.662	0.662
	(4→4)–(6→6)	0.128	0.132

[a] $\chi_{aa}^N = 2.450$, $\chi_{bb}^N = 0.685$, $\chi_{aa}^D = 0.0$, $\chi_{bb}^D = -0.100$ MHz.

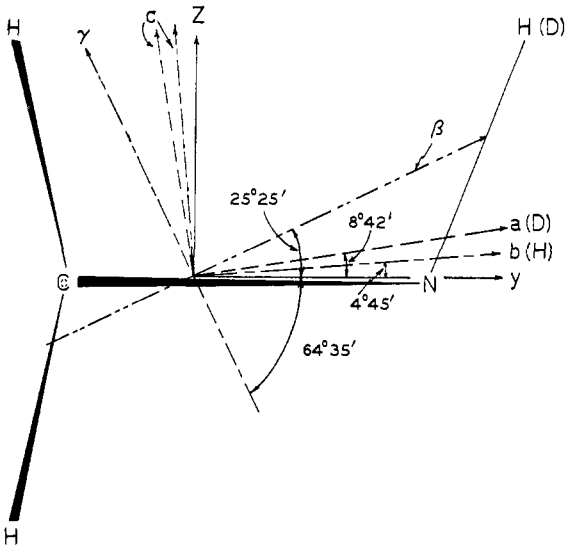

Figure 2. Ethylenimine showing the various axis systems described in the text.

^{14}N Field Gradient Tensor and the Local Electron Density

In the previous section we listed the diagonal elements of the ^{14}N quadrupole coupling constant tensor in two different principal inertial axis systems. The results are summarized in Table III. As shown in Figure 2, the *a* principal inertial axis in ethylenimine-d_1 is 8° 42′ above the plane of the molecule. In ethylenimine the *b* axis is 4° 45′ above the plane (adding deuterium causes an interchange of the *a* and *b* axes.) The unitary transformations relating the ^{14}N nuclear quadrupole coupling constant tensors in the two principal inertial axes (related by $\theta = 3° 57'$) are given in eq 1.

Table III. Nonzero Elements of the ^{14}N Quadrupole Coupling Constant Tensors for Ethylenimine and Ethylenimine-d_1[a]

$\chi_{aa}(H) = 0.685 \pm 0.005$	$\chi_{aa}(D) = 2.450 \pm 0.005$
$\chi_{bb}(H) = 2.170 \pm 0.005$	$\chi_{bb}(D) = 0.685 \pm 0.005$
$\chi_{cc}(H) = -2.855 \pm 0.005$	$\chi_{cc}(D) = -3.135 \pm 0.005$
$\chi_{bc}(H) = 2.210 \pm 0.08$	$\chi_{ac}(D) = 1.844 \pm 0.08$

[a] All values are in megahertz.

$$\chi^H = \underset{\sim}{R}\underset{\sim}{T}\chi^D\underset{\sim}{T}\underset{\sim}{R} \qquad (1)$$

$$\underset{\sim}{R} = \begin{pmatrix} 1 & 0 & 0 \\ 0 & \cos\theta & \sin\theta \\ 0 & -\sin\theta & \cos\theta \end{pmatrix}; \quad \underset{\sim}{T} = \begin{pmatrix} 0 & 1 & 0 \\ -1 & 0 & 0 \\ 0 & 0 & 1 \end{pmatrix}$$

(8) W. H. Flygare, *J. Chem Phys.*, 41, 206 (1964).
(9) G. Erlandsson and W. Gordy, *Phys. Rev.*, 106, 513 (1957).

χ^H and χ^D are the ^{14}N nuclear quadrupole coupling tensors in ethylenimine and ethylenimine-d_1, respectively, as listed in Table III. Owing to molecular symmetry, the only nonzero off-diagonal elements in χ^D or χ^H are $\chi_{ac}{}^D$ and $\chi_{bc}{}^H$ (see Figure 2). Solving eq 1 for the off-diagonal elements gives

$$\chi_{ac}{}^D = \frac{\chi_{cc}{}^H - \chi_{aa}{}^H \sin^2\theta - \chi_{cc}{}^D \cos^2\theta}{2 \cos\theta \sin\theta} \quad (2)$$

$$\chi_{bc}{}^H = \chi_{ac}{}^D[\cos^2\theta - \sin^2\theta] + [\chi_{aa}{}^D - \chi_{cc}{}^D] \sin\theta \cos\theta \quad (3)$$

Substituting $\theta = 3° 57'$ and the results in Table III into eq 2 and 3 gives

$$\chi_{ac}{}^D = 1.844 \pm 0.08 \text{ MHz}$$
$$\chi_{bc}{}^H = 2.210 \pm 0.08 \text{ MHz} \quad (4)$$

The final results are listed in Table III. Both of the χ^D and χ^H tensors can be diagonalized to yield the values in the principal field gradient axis system (the nuclear quadrupole moment is a constant). A counterclockwise rotation of 20° 40′ diagonalizes χ^H and a counterclockwise rotation of 16° 43′ diagonalizes χ^D. The elements in the principal field gradient axis system are given in Table IV. The orientation of the principal field gradient tensor is also shown in Figure 2. The principal field gradient quadrupole coupling constant tensor elements are $\chi_{\alpha\alpha} = 0.685 \pm 0.005$ MHz, $\chi_{\beta\beta} = 3.004 \pm 0.09$ MHz, and $\chi_{\gamma\gamma} = -3.689 \pm 0.09$ MHz.

Table IV. ^{14}N Nuclear Quadrupole Coupling Constants in the Principal Field Gradient Axis System Calculated for Both Ethylenimine and Ethylenimine-d_1[a]

	Coupling constants, MHz	
	C_2H_4NH	C_2H_4ND
$\chi_{\alpha\alpha}$	0.685 ± 0.005	0.685 ± 0.005
$\chi_{\beta\beta}$	3.004 ± 0.09	3.002 ± 0.09
$\chi_{\gamma\gamma}$	−3.689 ± 0.09	−3.687 ± 0.09

[a] The β principal field gradient axis is 25° 25′ ± 30′ above the molecular plane (see Figure 2).

The γ axis approximates the C_3 axis in NH_3 ($\chi_{\gamma\gamma} = -4.08$ MHz),[10] $H_3CC{\equiv}N$ ($\chi_{\gamma\gamma} = -4.21$ MHz),[10] or $F_3CC{\equiv}N$ ($\chi_{\gamma\gamma} = -4.70$ MHz).[10] However, the large asymmetry in $\chi_{\alpha\alpha}$ and $\chi_{\beta\beta}$ indicates a dramatic breakdown of the C_3 symmetry in the principal field gradient axis system of ethylenimine. The same breakdown of C_3 symmetry (but with the opposite sign) in the principal field gradients has been observed in difluoroamine.[11] The principal field gradient axis system in F_2NH has nearly the same orientation with respect to the FNF plane as in ethylenimine (compare Figure 1 in ref 11 with Figure 2 in this paper). However, the FNF angle is 102.9° and the NCN angle is less than 60°. Results similar to F_2NH have been observed in F_2NCH_3.[12]

The principal ^{14}N field gradient tensor can be rotated clockwise by 25° 25′ to give the field gradient elements in the molecular plane. The results are shown in Table V.

(10) C. H. Townes and A. L. Schawlow, "Microwave Spectroscopy," McGraw-Hill Book Co., Inc., New York, N. Y., 1955.
(11) D. R. Lide, Jr., *J. Chem. Phys.*, **38**, 456 (1963).
(12) L. Pierce, R. G. Hayes, and J. F. Beecher, *ibid.*, **46**, 4352 (1967).

Table V. Nonzero Elements of the ^{14}N Nuclear Quadrupole Coupling Constant Tensor in the Molecular Axis System (See Figure 2[a])

χ_{xx}	0.685 ± 0.005
χ_{yy}	1.77 ± 0.16
χ_{zz}	−2.46 ± 0.16
χ_{yz}	2.59 ± 0.13

[a] All numbers are listed in units of megahertz.

The ^{14}N nuclear quadrupole moment is known to be[10]

$$Q = \langle n|\sum_i e_i(3z_i^2 - r_i^2)|n\rangle = 0.077 \times 10^{-34} \text{ esu cm}^2$$

where n represents the nuclear wave function and the sum over i is over all nuclear charges in the ^{14}N nucleus. Thus the values of the ^{14}N field gradients divided by $e = -4.8 \times 10^{-10}$ esu in the planar axis system are (see Figure 2)

$$\frac{q_{xx}}{e} = \left(\frac{3x^2 - r^2}{r^5}\right)_{av} = -1.23 \times 10^{24} \text{ cm}^{-3}$$
$$\frac{q_{yy}}{e} = \left(\frac{3y^2 - r^2}{r^5}\right)_{av} = -3.16 \times 10^{24} \text{ cm}^{-3} \quad (5)$$
$$\frac{q_{zz}}{e} = \left(\frac{3z^2 - r^2}{r^5}\right)_{av} = 4.39 \times 10^{24} \text{ cm}^{-3}$$
$$\frac{q_{yz}}{e} = 3\left(\frac{yz}{r^5}\right)_{av} = -4.62 \times 10^{24} \text{ cm}^{-3}$$

We will use the same approach in the present work on ethylenimine as we used previously in ethylene sulfide in order to compute the field gradients. The main assumption in this approach is that the field gradients are caused only by the nitrogen localized atomic orbitals. Each nitrogen orbital is occupied by a certain fraction of two electrons. The assumption of local field gradients appears to be strengthened on the basis of recent work on *trans*-propylenimine.[13] The effect of the additional methyl group in *trans*-propylenimine relative to ethylenimine appears to have a minor effect on the field gradients in any common axis system. Similar conclusions have been obtained in methyl ethylenimine.[14]

Referring to Figure 2, we can write the local nitrogen atomic 2p hybrid orbitals as shown in Table VI. ψ_1, ψ_2, and ψ_4 are sp^2 hybrids and ψ_2 contains a lone pair of

Table VI. Walsh Bonding Scheme for Ethylenimine

Function	No. of electrons
$\psi_1 = \frac{1}{\sqrt{3}}\chi_{2s} + \frac{1}{\sqrt{6}}\chi_{2p_y} + \frac{1}{\sqrt{2}}\chi_{2p_z}$	n_H
$\psi_2 = \frac{1}{\sqrt{3}}\chi_{2s} + \frac{1}{\sqrt{6}}\chi_{2p_y} - \frac{1}{\sqrt{2}}\chi_{2p_z}$	2
$\psi_3 = \chi_{2p_x}$	n_x
$\psi_4 = \frac{1}{\sqrt{3}}\chi_{3s} - \sqrt{\frac{2}{3}}\chi_{2p_y}$	n_y

electrons. ψ_1 and ψ_2 are directed away from the ring with the $\psi_1 N \psi_2$ plane perpendicular to the plane of the ring. ψ_1 is the nitrogen part of the NH bond and ψ_4

(13) Y. S. Li, M. D. Harmony, D. Hayes, and E. L. Beeson, Jr., *ibid.*, **47**, 4514 (1967).
(14) M. D. Harmony and M. Sancho, *ibid.*, **48**, 1911 (1968).

is the third sp^2 hybrid directed into the ring. ψ_3 is the unhybridized $2p_y$ orbital which is in the plane of the ring and perpendicular to the sp^2 plane. n_H is the number of electrons near the nitrogen atom in the NH bond. n_x is the number of electrons in the $2p_x$ orbital and n_y is the number of electrons in the sp^2 hybrid directed into the ring.

The 2p-type atomic orbitals in Table VI are written as

$$\begin{aligned}\chi_{2p_x} &= \frac{1}{\sqrt{2}}[Y_1^1 + Y_{-1}^1]\phi_{2p}(r)\\ \chi_{2p_y} &= \frac{1}{i\sqrt{2}}[Y_1^1 - Y_{-1}^1]\phi_{2p}(r)\\ \chi_{2p_z} &= Y_0^1\phi_{2p}(r)\\ \phi_{2p}(r) &= \frac{1}{\sqrt{6}}(2\xi)^{3/2}\xi r e^{-\xi r}\end{aligned} \tag{6}$$

We can now combine the functions in eq 6 and Table VI with the operators in eq 5 to compute three independent field gradient parameters. The values of the necessary matrix elements which are nonzero are

$$\begin{aligned}\langle\chi_{2p_z}|(q_{zz}/e)|\chi_{2p_z}\rangle &= \frac{4}{5}\left(\frac{1}{r^3}\right)_{av}\\ \langle\chi_{2p_y}|(q_{zz}/e)|\chi_{2p_y}\rangle &= -\frac{1}{2}\left[\frac{4}{5}\left(\frac{1}{r^3}\right)_{av}\right]\\ \langle\chi_{2p_x}|(q_{zz}/e)|\chi_{2p_x}\rangle &= -\frac{1}{2}\left[\frac{4}{5}\left(\frac{1}{r^3}\right)_{av}\right]\end{aligned} \tag{7}$$

and cyclic permutations. The off-diagonal element is given by

$$\langle\chi_{2p_y}|(q_{yz}/e)|\chi_{2p_z}\rangle = \frac{3}{5}\left(\frac{1}{r^3}\right)_{av} \tag{8}$$

$(1/r^3)_{av}$ is the average value of $1/r^3$ using the normalized radial function in eq 6. The values of the three independent field gradients are

$$\begin{aligned}(q_{yy}/e) &= \frac{1}{15}\left(\frac{1}{r^3}\right)_{av}[8n_y - n_H - 2 - 6n_x] = \\ &\qquad -3.16 \times 10^{24}\ \text{cm}^{-3}\\ (q_{zz}/e) &= \frac{1}{15}\left(\frac{1}{r^3}\right)_{av}[-4n_y + 5n_H + 10 - 6n_x] = \\ &\qquad 4.39 \times 10^{24}\ \text{cm}^{-3}\\ (q_{yz}/e) &= \frac{6}{5\sqrt{12}}\left(\frac{1}{r^3}\right)_{av}[n_H - 2] = \\ &\qquad -4.62 \times 10^{24}\ \text{cm}^{-3}\end{aligned} \tag{9}$$

We will use the free atom value of $(1/r^3)_{av}$ to fix the radial function. The result is

$$\left(\frac{1}{r^3}\right)_{av}^{N} = 16.6 \times 10^{24}\ \text{cm}^{-3} \tag{10}$$

The value of n_H can be determined solely with q_{yz}/e. Substituting eq 10 into q_{yz}/e of eq 9 gives the value of n_H. The result is

$$n_H = 1.20 \tag{11}$$

This appears to be a reasonable number in light of the apparent polarity of the N–H bond. Substituting $n_H = 1.20$ into q_{yy}/e and q_{zz}/e in eq 9 allows a determination of n_y and n_x. The final results are

$$\begin{aligned}n_H &= 1.20\\ n_y &= 1.03\\ n_x &= 1.32\end{aligned} \tag{12}$$

Thus, although ψ_4 in Table VI has less electrons associated with it than ψ_3, the directed nature of ψ_4 gives a local electron distribution with a maximum pointing toward the center of the ring. The same relative distribution of electrons in the ring was observed in ethylene sulfide.[2]

It is interesting to point out that the value of (q_{yz}/e) in eq 9 is a useful criterion for the hybrid character of the orbitals. It is clear that if ψ_1 in eq 6 also contained a lone pair ($n_H = 2.0$) as in ethylene sulfide, the value of q_{yz}/e would be zero. In ethylenimine, however, the value of q_{yz}/e is determined from the hybridization coefficients and n_H. As the amount of p character in ψ_1 and ψ_2 in Table VI increases, the value of n_H must also increase.

Consider a general set of hybrids as shown in Table VII. These orbitals are defined in a manner similar to the sp^2 orbitals in Table VI. A is a general hybridization factor. The independent field gradients computed with these functions are

Table VII. Coulson–Moffitt Types of Hybrid Orbitals

Function	No. of electrons in orbital
$\psi_1 = \left(\frac{1}{2} - A^2\right)^{1/2}\chi_{2s} + \frac{1}{\sqrt{2}}\chi_{2p_x} + A\chi_{2p_y}$	n_H (NH bond)
$\psi_2 = \left(\frac{1}{2} - A^2\right)^{1/2}\chi_{2s} - \frac{1}{\sqrt{2}}\chi_{2p_x} + A\chi_{2p_y}$	2 (lone pair)
$\psi_3 = A\chi_{2s} + \frac{1}{\sqrt{2}}\chi_{2p_x} - \left(\frac{1}{2} - A^2\right)^{1/2}\chi_{2p_y}$	n_{CN} (C_1N bond)
$\psi_4 = A\chi_{2s} - \frac{1}{\sqrt{2}}\chi_{2p_x} - \left(\frac{1}{2} - A^2\right)^{1/2}\chi_{2p_y}$	n_{CN} (C_2N bond)

$$\begin{aligned}(q_{xx}/e) &= \frac{4}{5}\left(\frac{1}{r^3}\right)_{av}\left\{(n_H + 2)\left(-\frac{1}{4} - A^2\right) + n_{CN}\left(\frac{1}{2} + 2A^2\right)\right\}\\ (q_{yy}/e) &= \frac{4}{5}\left(\frac{1}{r^3}\right)_{av}\left\{(n_H + 2)\left(-\frac{1}{4} + A^2\right) + n_{CN}\left(\frac{1}{2} - 2A^2\right)\right\}\\ (q_{zz}/e) &= \frac{4}{5}\left(\frac{1}{r^3}\right)_{av}\left\{(n_H + 2)\left(\frac{1}{2} - \frac{A}{2}\right)^2 - n_{CN}(1 - A^2)\right\}\\ (q_{yz}/e) &= \frac{3}{5}\left(\frac{1}{r^3}\right)_{av}\left\{(n_H - 2)\left(\frac{2}{\sqrt{2}A}\right)\right\}\end{aligned} \tag{13}$$

Using the numbers in eq 5 and 10 there is no solution of eq 13 with A varying from 0 to $1/\sqrt{2}$. Thus the hybrids

defined in Table VII will not fit the field gradients. This includes the choice of $A = 1/\sqrt{6}$ which is the case of two equivalent sp^5 hybrids in the plane for the CN bonds. A linear combination of ψ_1 and ψ_2 in Table VI (Walsh orbitals) will also yield sp^5 orbitals in the molecular plane. These orbitals are equivalent to ψ_3 and ψ_4 in Table VII when $A = 1/\sqrt{6}$.

In summary, we have tried to fit the ^{14}N field gradients in ethylenimine with two sets of local orbitals. The Walsh orbitals have two sp^2 types of orbitals directed away from and perpendicular to the ring; one of these orbitals contains the NH bond and the other contains the lone pair. The third sp^2 is directed into the ring and a fourth orbital is a pure p orbital which is perpendicular to the sp^2 plane. The Coulson–Moffitt orbitals employ two variable hybrids perpendicular to and away from the ring and two equivalent orbitals in the molecular plane. The requirement that the Coulson–Moffitt orbitals in the plane are equivalent (by symmetry) does not allow enough flexibility to fit the local field gradients. The additional flexibility in the Walsh scheme with two inequivalent in-plane orbitals allows a satisfactory fit.

Barrier to Inversion

In the Experimental Section we were able to place an upper limit on the tunneling frequency of the proton at 15 kHz. We would now like to make an estimate of the minimum barrier height to give this splitting. We will assume the potential function for the proton bending vibration to be a sum of a quartic minus a harmonic component

$$V(s) = ks^4 - k's^2 \tag{14}$$

where s is the displacement of the proton from the CNC plane, k is the quartic potential force constant, and k' is the harmonic force constant. The maximum potential is at $s = 0$. The minima on either side of the

$$V_{max} = V(s = 0) = 0 \tag{15}$$

plane are easily obtained from eq 14. The result is

$$s_m = \pm\sqrt{\frac{k'}{2k}} \tag{16}$$

Thus the potential energy at the minima is

$$V_{min} = V(s_m) = -\frac{1}{4}\left(\frac{k'}{k}\right)^2 \tag{17}$$

and the resultant barrier height, V, is

$$V = V_{max} - V_{min} = \frac{1}{4}\left(\frac{k'}{k}\right)^2 \tag{18}$$

If we assume the value of V is high relative to the vibrational spacings, we can expand $V(s)$ in eq 14 to give a harmonic potential for the bending mode of the proton (with respect to the plane) on either side of the barrier. This is achieved by a Taylor series expansion about s_m

$$V(s) = V(s_m) + V'(s_m)[s - s_m] + \frac{V''(s_m)}{2}[s - s_m]^2 + \dots$$

$$V(s) = V + 2k'(s - s_m)^2 + \dots \tag{19}$$

where each prime indicates a derivative with respect to s. V is given in eq 18 and s_m is given in eq 16. Thus if we retain only terms up to $(s - s_m)^2$ in eq 19, we have a harmonic oscillator on each side of the molecular plane with energies given by

$$E_v(n) = \epsilon_v\left(n + \frac{1}{2}\right) - V$$

$$\epsilon_v = 2\hbar\sqrt{\frac{k'}{\mu}} \tag{20}$$

where μ is the reduced mass for the proton bending mode. If the barrier is high as is assumed, the states given in eq 20 are all doubly degenerate. The normalized wave function for the doubly degenerate ground state is

$$\psi = \frac{\gamma^{1/2}}{\pi^{1/4}} e^{-(\gamma/2)(s-s_m)^2} \tag{21}$$

$$\gamma = \left(\frac{\sqrt{4\mu k'}}{h}\right)^{1/2} \tag{22}$$

The values of $s_m = \pm k'/2k$ give the function for either side of the molecular plane. If the barrier height is infinitely high, the harmonic oscillators, described by eq 21 on either side of the molecular plane, do not overlap and there is no penetration of the barrier (tunneling). This is the case of perfectly doubly degenerate states on either side of the barrier. However, if the barrier height is finite, the functions overlap and tunneling is possible. The overlap breaks the degeneracy and the energy spacings between the originally doubly degenerate levels divided by Planck's constant yield the tunneling frequency. The secular equation describing the effects of a finite barrier on an originally degenerate high barrier system is

$$\begin{vmatrix} \alpha - \lambda & \beta - \lambda S \\ \beta - \lambda S & \alpha - \lambda \end{vmatrix} = 0 \tag{23}$$

where α is the original energy of the ground state on either side of the barrier. β is the matrix element of the complete Hamiltonian

$$\mathcal{H} = -\frac{\hbar^2}{2\mu}\frac{d^2}{ds^2} + 2k'(s - s_m)^2 - V \tag{24}$$

describing the proton bending motion. S in eq 23 is the overlap between the functions (eq 21) on either side of the barrier. The values of the matrix elements are

$$S = e^{-8V/\epsilon_v}$$

$$\alpha = E_v + (\epsilon_v/4) + 16V \tag{25}$$

$$\beta = S\alpha - 12SV$$

The solution to the secular equation yields two roots

$$\lambda_1 = \alpha - 12SV$$

$$\lambda_2 = \alpha + 12SV \tag{26}$$

Thus as a result of the finite barrier, V, the doubly degenerate ground state, is now split by an energy $\lambda_2 - \lambda_1$ giving a tunneling frequency of

$$\nu = \frac{\Delta E}{h} = \frac{\lambda_2 - \lambda_1}{h} = \frac{1}{h}(24SV) = \frac{1}{h}(24Ve^{-8V/\epsilon_v}) \tag{27}$$

This formula is convenient for determining the barrier height as a function of ϵ_v and the tunneling frequency, ν. Using an upper limit for ν of 15 kHz, and ϵ_v = 1209 cm^{-1} for the HN bending mode in ethylenimine,[15] gives a lower limit to V.

$$V = 4065 \text{ cm}^{-1} = 11.6 \text{ kcal} \quad (28)$$

This lower limit for the barrier height is very close to the activation energy of 11.0 (11.9) kcal for nitrogen inversion (or proton tunneling) in 2,2,3,3-tetramethylaziridine (tetramethylethylenimine).[16] As we have found the tunneling frequency to be low, it is likely that tunneling adds little to the measured rates in the magnetic resonance experiments. Therefore, the measured activation energy is likely to be a good measure of the barrier height. Our upper limit for V in ethylenimine is, however, much lower than given in a recent calculation (34 kcal).[17]

We can now define the potential constants in $V(s)$ in eq 14. It is also necessary to list the reduced mass which we assume is equal to the proton mass.

$$k = 1.45 \times 10^{20} \text{ ergs/cm}^4$$

$$k' = 2.17 \times 10^{6} \text{ ergs/cm}^2$$

$$s_m = \pm 0.86 \times 10^{-8} \text{ cm}$$

Acknowledgment. The support of the National Science Foundation is gratefully acknowledged.

(15) H. T. Hoffman, Jr., G. E. Evans, and G. Glockler, *J. Am. Chem. Soc.*, 73, 3028 (1951).
(16) T. J. Burdos, C. Szantay, and C. K. Havada, *ibid.*, 87, 5796 (1965).
(17) G. W. Koeppl, D. S. Sagatys, and G. S. Krishnamurthy, *ibid.*, 89, 3396 (1967).

Free Radical Addition of Trifluoroacetonitrile to Propylene[1]

B. Hardman and G. J. Janz[2]

Contribution from the Department of Chemistry, Rensselaer Polytechnic Institute, Troy, New York 12181. *Received May 25, 1968*

Abstract: A study is reported of the rate of the gas-phase addition of CF_3CN to propylene over the range 400–450°. Under conditions such that $CF_3CN \gg C_3H_6$, the rate equation is $\partial[CF_3(C_3H_6)CN]/\partial t = 10^{14\pm2}\exp(-51.5/RT)[CF_3CN][C_3H_6]$ l. mol^{-1} sec^{-1}. The results are consistent with a free radical mechanism in which the initiation step is bimolecular, $CF_3CN + C_3H_6 \rightarrow CF_3 + C_3H_6CN$, and in which chain termination is due to hydrogen abstraction from C_3H_6 by trifluoromethyl radicals.

The telomerization of CF_3I with ethylene has been investigated in the homogeneous gas phase (309°) by Bell.[3] A similar study, but with CF_3CN and C_2H_4, in the range 365–445° was reported by Flannery and Janz,[4] the rate equation being

$$\partial[CF_3CH_2CH_2CN]/\partial t = 10^{7.0\pm0.4}\exp(-27 \pm 3/RT) \times [CF_3CN][C_2H_4] \text{ l. mol}^{-1} \text{ sec}^{-1} \quad (1)$$

under conditions of excess CF_3CN (as required to minimize the formation of telomers[5]). The present communication reports the results of a study of the addition of CF_3CN to C_3H_6, under conditions such that $CF_3CN \gg C_3H_6$. With propylene two addition products could be expected under such conditions. The structures of these compounds and the relative amounts were explored; these have been reported elsewhere.[6] Thus at 400°, it was found that both the 1:1 adducts $CF_3CH_2CH(CN)CH_3$ (I) and $NCCH_2CH(CF_3)CH_3$ (II) were present in the product, with I being predominant (89 ± 1%) in the mixture. When vinyl fluoride is used as the olefin,[7] this addition reaction yields essentially $CF_3CH_2CH(CN)F$. These results are consistent with CF_3 radicals as the primary chain carrier, as was proposed in our earlier work with CF_3CN and ethylene.[4,5,7]

With knowledge of the structures of the products from the addition of CF_3CN to propylene, a quantitative study of the reaction energetics appeared feasible. The results of such an investigation are given in this communication.

Experimental Section

The apparatus and procedure were those described in detail in our earlier paper.[5]

The reactants, CF_3CN (Peninsular Chemical Research, Inc., 95% minimum purity) and C_3H_6 (Matheson Co., Inc., 99% minimum purity), were degassed under high vacuum and triply distilled at low temperature prior to use.

Kinetic data were obtained by manometric techniques. The over-all rate was monitored up to 40–50% conversions, relative to the initial olefin concentration. The total initial pressures ranged from 0.50 to 0.85 atm. For each experiment the initial reactant ratio (CF_3CN/C_3H_6) was adjusted to be from 8.5 to 8.9, this being the upper limit for excess of nitrile at which quantitative measurements of the addition products could be gained with our analytical facilities. A large excess of nitrile is important in order to minimize the formation of telomeric adducts other than the 1:1 addition compounds. The analyses of the gaseous and liquid products were by gas chromatography and infrared spectroscopy.

In the gaseous fraction, unconverted CF_3CN and C_3H_6 and small amounts of CF_3H (typically ~1.0 mol %) were observed. No evidence was found for the formation of C_2F_6, HCN, $(CN)_2$, or gaseous compounds that would arise from propylene pyrolysis.

(1) Based in part on a thesis submitted by B. H. in partial fulfillment of the requirements for the Ph.D. degree, June 1968, Rensselaer Polytechnic Institute.
(2) To whom all correspondence should be addressed.
(3) T. N. Bell, *J. Chem. Soc.*, 4973 (1961).
(4) J. B. Flannery and G. J. Janz, *J. Am. Chem. Soc.*, 88, 5097 (1966).
(5) N. A. Gac and G. J. Janz, *ibid.*, 86, 5059 (1964).
(6) G. J. Janz, N. A. Gac, A. R. Monahan, and W. J. Leahy, *J. Org. Chem.*, 30, 2075 (1965).
(7) G. J. Janz and J. B. Flannery, *J. Phys. Chem.*, 70, 2861 (1966).